Turkish Journal of Electrical Engineering & Computer Sciences

http://journals.tubitak.gov.tr/elektrik/

Research Article

Turk J Elec Eng & Comp Sci
(2014) 22: 1367 – 1381
© TÜBİTAK
doi:10.3906/elk-1210-24

A novel fuzzy filter for speckle noise removal

Mehmet Ali SOYTÜRK[1], **Alper BAŞTÜRK**[2], **Mehmet Emin YÜKSEL**[3,*]
[1]Department of Aircraft Electrics and Electronics, Civil Aviation School, Erciyes University, Kayseri, Turkey
[2]Department of Computer Engineering, Faculty of Engineering, Erciyes University, Kayseri, Turkey
[3]Department of Biomedical Engineering, Faculty of Engineering, Erciyes University, Kayseri, Turkey

Received: 05.10.2012 • **Accepted:** 25.01.2013 • **Published Online:** 15.08.2014 • **Printed:** 12.09.2014

Abstract: In this paper, a novel fuzzy system-based method for speckle noise removal is proposed. The proposed method consists of a fuzzy inference system, an edge detection and dilation unit, and an image combiner. The fuzzy inference system includes 5 inputs and 1 output, and it is responsible for filtering the speckle noisy image. The inputs of the fuzzy system consist of the center pixel of the filtering window and its 2 horizontal and vertical neighbors. The edge detection and dilation unit is used for classifying the uniform areas and nonuniform image regions such as edges. The image combiner unites the output images filtered 1 and 2 times according to the information coming from the edge detection and dilation unit. The training phase of the fuzzy inference system is implemented using the clonal selection optimization algorithm with appropriate training data. The performance of the proposed method is compared with popular speckle noise removal filters available in the literature by performing extensive simulations. The experimental results show that the proposed method can significantly reduce the speckle noise from digital images while preserving edges, textures, and valuable details.

Key words: Speckle noise filtering, fuzzy inference system, image processing

1. Introduction

In many imaging systems, acquired images are corrupted since they are affected by various corruptive factors. Noise is the most common corruptive factor and causes undesirable changes of the pixel values in various amounts or variances. There are different kinds of noise models in the field of signal and image processing to model and study the effects of real noise. One of those models is the speckle noise model, which is a locally correlated multiplicative noise. In this model, the image quality is considerably degraded since the pixel values in the image are multiplied with the noise components. The basic properties of the speckle noise were defined by Goodman [1] and a general model for the speckle noise was presented by Jain [2]. Many imaging systems, such as synthetic aperture radar (SAR), ultrasound, or laser, suffer from speckle noise. In such systems, speckle noise inherently occurs as a result of the interference of the reflected signal by object surface. Almost all pixels in the acquired image are affected by the speckle noise and this effect causes a freckled appearance and low resolution quality. The aim of a speckle noise reduction filter is to strongly smooth the uniform areas without losing useful information in the nonuniform areas (i.e. edges) of the input image [3].

Many methods have been proposed in the literature to reduce the speckle noise in digital images. Some of these methods use local statistics, such as the Lee minimum mean square error (MSE) filter (Lee MMSEF) [4], Frost filter (FROSTF) [5], and Kuan filter [6,7]. The concept of the local variance and mean proposed

*Correspondence: yuksel@erciyes.edu.tr

by Wallis [8] was used in the Lee MMSEF for additive and multiplicative noise removal. The Kuan filter is a general form of the Lee MMSEF. The only difference between the Kuan filter and the Lee MMSEF is the weighting function, which is a scaling factor of the difference between the center pixel and the mean of the filtering window. Improved results are obtained through these filters by adding the scaled value to the mean of the filtering window. In the FROSTF, averaging or all-pass filter operation is achieved by an exponential convolution kernel that can change its behavior between the average filter and the identity filter. While the FROSTF acts as a mean filter in uniform areas by a low coefficient value, it acts as an all-pass filter with a high coefficient value in the nonuniform areas to preserve edge features.

An extended version of the Lee MMSE and the FROSTFs proposed by Lopez et al. consisted of 3 cases with different thresholds [9,10]. In this method, mean filtering is applied when the local rate of statistics is below a lower threshold and all-pass filtering is applied when this statistic is above a higher threshold. However, the method acts as standard Lee MMSE and/or FROSTF when the local rate of statistics is between these 2 thresholds.

Another method for speckle noise removal was presented by Perona and Malik [11], which used the anisotropic diffusion filter (ADF) for smoothing the image. In this method, different diffusion rates are used, depending on the image regions, in order to restrict diffusion on the edges and preserve image details. Since the diffusion coefficient is small in the vicinity of the edges, the ADF acts as an all-pass filter and preserves image details. On the contrary, the diffusion coefficient is large for the other areas; therefore, the ADF acts as a Gaussian filter for smoothing. The anisotropic diffusion approach was improved by Yu and Acton [3]. In this method, called the speckle-reducing ADF (SRADF), the diffusion coefficient is readjusted in each loop according to current gradient and current local statistics, as in the Lee MMSEF. The deficiency of the anisotropic diffusion approach for multiplicative speckle noise is successfully removed by this method.

An extended form of the SRADF was presented by Krissian et al. [12] that combined a flux-based matrix diffusion method [13,14] and the detail-preserving anisotropic diffusion method proposed by Aja-Fernandez et al. [15]. In this method, the matrix diffusion approach is used instead of scalar diffusion in order to enable multilevel filtering.

The recently proposed Lee improved sigma filter (Lee ISF) [16] for speckle noise removal in SAR data is actually a modified form of the sigma filter that was previously presented by Lee [17,18]. In the simple sigma filter, almost all pixels in the local region are included within a 2-sigma range from its mean, while the 2-sigma range is readjusted in the Lee ISF to maintain the mean value after pixel selection, and then the Lee MMSEF is applied to the filtering window with new variance and mean values.

In recent years, some fuzzy logic-based methods have been used for speckle noise removal. One of these methods was proposed by Puvanathasan et al., in which the fuzzy anisotropic diffusion method was used to adjust the diffusion coefficients with type-2 fuzzy reasoning [19]. In this method, a big diffusion rate is used in the uniform areas and the diffusion rate is reduced for nonuniform areas (e.g., edges) since the difference between the neighbor pixel values is large. In another work by Puvanathasan et al., type-2 fuzzy reasoning approaches were used for the soft threshold of wavelet coefficients [20]. Another fuzzy logic-supplemented approach for speckle noise removal was presented by Zhang et al. [21]. In this approach, the normalized image was mapped to the fuzzy domain using maximum fuzzy entropy and then the fuzzy fractional anisotropic diffusion approach was used for the fine tuning process. Fuzzy logic-based methods have also been successfully applied for impulse noise removal [22–27].

Many other recent despeckling methods have been effectively used in different ways to remove speckle noise from digital images in the literature [28–33]. An algorithm based on multiscale curvelet analysis was used in [28] for speckle noise reduction in SAR images. In [29], a nonlinear diffusion filter with anisotropic behavior was used for denoising speckled images. A hybrid technique with anisotropic diffusion was used in [30]. A combination of the Daubechies–Wiener methods was used in the hybrid technique for speckle removal from ultrasound images. To suppress the speckle effect in the optical coherence tomography images, a 2-dimensional CCD camera was used in [31] for a single lateral point from multiple spectral interference data. An algorithm based on the 2-sided generalized gamma distribution model was used in [32] for speckle noise removal from SAR images. In [33], some prominent denoising methods for ultrasound enhancement were classified as preprocessing and postprocessing and were examined for performance analysis.

In this paper, a new fuzzy system-based method for speckle noise removal is proposed. With this method, an efficient speckle noise removal based on a type-1 fuzzy inference system is obtained without any diffusion or image transform approach. The remainder of the paper is as follows. Some of the popular speckle noise removal filters available in the literature are mentioned in Section 2. These filters are used as competing filters to evaluate the performance of the proposed filter. The fuzzy inference system and optimization algorithm used in the proposed method are mentioned in Sections 3 and 4, respectively. The construction, training, and implementation of the proposed method are explained in Section 5. The results of the filtering experiments performed to evaluate the performance of the proposed method and competing operators are reported and discussed in Section 6. The discussion and conclusion are presented in Section 7.

2. Available methods in the literature

The most recognized speckle filters in the literature are probably the Lee MMSEF [4], FROSTF [5], ADF [11], SRADF [3], and Lee ISF [16]. These are explained briefly below.

2.1. Lee MMSEF

This filter uses local statistics and the minimum MSE approach to reduce speckle noise. Improved data are obtained by the following formulae:

$$\widehat{I}_p = I_m + \omega(I_p - I_m), \tag{1}$$

$$\omega = 1 - (C_I/C_W)^2, \tag{2}$$

where I_p is the center pixel value, $\widehat{I}_p$ is the improved center pixel value, I_m is the mean value of the filter window, ω is the weighting coefficient determined by Eq. (2), C_I is the ratio of the standard deviation and mean of the uniform areas of the input image, and C_W is the ratio of standard deviation and mean of the filter window. For uniform areas, ω converges to 0; hence, the filter output approaches the mean of the filtering window. In contrast to the previous case, ω converges to 1 for nonuniform areas. Therefore, the value of the center pixel does not greatly change and the edges remain unchanged.

2.2. Lee ISF

This filter attempts to avoid some of the drawbacks of the simple sigma filter [17,18] by using MMSE filter adaptation. First, the center pixel value of the 3 × 3 input window is estimated with a MMSE filter to determine the new sigma range. Next, the pixels within the new sigma range in a 9 × 9 filtering window are selected, and the new variance and mean values for the selected pixels in the filtering window are computed. Finally, the value of the center pixel is computed using the Lee MMSEF approach again.

2.3. FROSTF

This filter uses a convolution kernel that can smooth various regions of an image by using local statistics. The filter output is obtained by the following equations:

$$\widehat{I}_p = \frac{\sum\limits_{n \in W_p} \varepsilon_n I_n}{\sum\limits_{n \in W_p} \varepsilon_n}, \tag{3}$$

$$\varepsilon_n = \exp(-DC_W^2 d_n), \tag{4}$$

where I_n is the nth pixel value of the filtering window, D is the damping factor, and d_n are distances between the center pixel and the other pixels of the window. The value of the damping factor is selected so that the DC_W product converges to 0 for uniform areas and diverges from 0 for nonuniform areas.

2.4. ADF

This filter uses a divergence operator to smooth the image. Smoothing is controlled by a coefficient that is varied in connection with the image gradient for preserving image details. The anisotropic diffusion proposed by Perona and Malik [11] is explained with the following equations:

$$\begin{cases} \partial I/\partial t = div\,[c(|\nabla I|)\nabla I] \\ I(t=0) = I_0 \end{cases}, \tag{5}$$

$$c(a) = 1/(1 + a/\kappa)^2 \text{ or } \quad c(a) = \exp[-(a/\kappa)^2], \tag{6}$$

where div is the divergence operator, $|.|$ denotes the magnitude, $c(a)$ is the diffusion coefficient, ∇ is the gradient operator, I_0 is the initial image, and I is the improved output image.

2.5. SRADF

This filter combines the advantages of the classic statistical speckle filters and the anisotropic diffusion method by applying the instant variation calculation to anisotropic diffusion method for speckle noise removal. Given an original noisy image $I_0(x, y)$, an improved output image $I(x, y; t)$ is obtained by the following equations:

$$\begin{cases} \partial I(x,y;t)/\partial t = div\,[c(q)\nabla I(x,y;t)] \\ I(x,y;0) = I_0(x,y) \end{cases}, \tag{7}$$

$$c(q) = 1/(1 + [q^2(x,y;t) - q_0^2(t)] \,/\, [q_0^2(t)(1 + q_0^2(t))]), \tag{8}$$

$$q_0^2 = \, var[i(t)]/\, i_m(t)^2, \tag{9}$$

where $c(q)$ is the diffusion coefficient and $q(x, y; t)$, which is the instantaneous coefficient of variation in the SRADF, is an edge detection operator. $q(x, y; t)$ takes high values at the edges and low values in uniform areas. The speckle scale function $q_0(t)$ controls the amount of smoothing in the SRADF. $var[i(t)]$ and $i_m(t)$ are the intensity variance and mean of the uniform area at iteration t, respectively.

3. Fuzzy inference system

The fuzzy inference system used in the proposed method is a first-order Sugeno fuzzy model with 5 inputs and 1 output [34]. The type of the antecedent membership functions of the fuzzy system are chosen as *generalized bell*, whereas the type of consequent membership functions are chosen as *linear*. The rule base of the fuzzy system contains 10 fuzzy rules, as listed below.

$$
\begin{array}{l}
1.\ if\ \ (X_1 \in M_{11})\&(X_2 \in M_{12})\&(X_3 \in M_{13})\&(X_4 \in M_{14})\&(X_5 \in M_{15}) \\
\quad then\ \ Q_1 = d_{11}X_1 + d_{12}X_2 + d_{13}X_3 + d_{14}X_4 + d_{15}X_5 + d_{16} \\
\\
2.\ if\ \ (X_1 \in M_{21})\&(X_2 \in M_{22})\&(X_3 \in M_{23})\&(X_4 \in M_{24})\&(X_5 \in M_{25}) \\
\quad then\ \ Q_2 = d_{21}X_1 + d_{22}X_2 + d_{23}X_3 + d_{24}X_4 + d_{25}X_5 + d_{26} \\
\\
3.\ if\ \ (X_1 \in M_{31})\&(X_2 \in M_{32})\&(X_3 \in M_{33})\&(X_4 \in M_{34})\&(X_5 \in M_{35}) \\
\quad then\ \ Q_3 = d_{31}X_1 + d_{32}X_2 + d_{33}X_3 + d_{34}X_4 + d_{35}X_5 + d_{36} \\
\\
\qquad \vdots \qquad\qquad\qquad \vdots \qquad\qquad\qquad \vdots \\
\\
10.\ if\ (X_1 \in M_{101})\&(X_2 \in M_{102})\&(X_3 \in M_{103})\&(X_4 \in M_{104})\&(X_5 \in M_{105}) \\
\quad then\ \ Q_{10} = d_{101}X_1 + d_{102}X_2 + d_{103}X_3 + d_{104}X_4 + d_{105}X_5 + d_{106}
\end{array},
$$

Here, X_J are inputs of the fuzzy system, Q_k denotes the consequent membership function of the kth rule, and $M_{i,j}$ denotes the ith antecedent membership function of the jth input. The generalized bell-type membership function, which is used for input fuzzification, is described as follows:

$$M_{i,j}(x) = \frac{1}{1 + \left| \frac{x - a_{i,j}}{b_{i,j}} \right|^{2c_{i,j}}} \quad i = 1, .., 10 \text{ and } j = 1, .., 5. \tag{10}$$

Parameters a, b, c, and d determine the shape of the membership functions. These parameters are optimized by the training process, which will be discussed later.

The output of the fuzzy system is obtained by calculation of the weighted average of the individual rule outputs. The weighting factor of each rule ω_k is calculated by producing the memberships of the inputs. For this purpose, input values are first converted to fuzzy membership values by using antecedent membership functions. Next, the *AND (&)* operator, which corresponds to the multiplication, is applied to these membership values. Hence, the weighting factor of each rule is calculated by:

$$\omega_k = M_{k1}(X_1)M_{k2}(X_2)M_{k3}(X_3)M_{k4}(X_4)M_{k5}(X_5) = \prod_{j=1}^{5} M_{kj}(X_j). \tag{11}$$

After obtaining the weighting factors, the output of the fuzzy system is calculated by the weighted average of the individual rule outputs as follows:

$$Y = \frac{\sum_{k=1}^{10} \omega_k Q_k}{\sum_{k=1}^{10} \omega_k}. \tag{12}$$

4. The clonal selection optimization algorithm

The clonal selection optimization algorithm (CSOA) was inspired by the clonal selection principle of the human immune system [35]. It searches for the global optimum without getting stuck at any local optimum. The CSOA is especially successful in optimization problems that have too many parameters. Therefore, it has been used in many engineering problems in practical applications. The block diagram of the CSOA is shown in Figure 1.

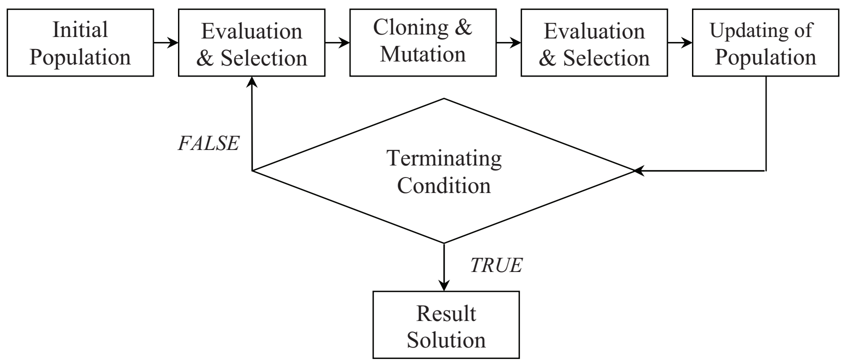

Figure 1. Block diagram of the CSOA.

In the CSOA, the initial population N is produced randomly. Each possible solution is represented by a cell and the problem for the algorithm is represented by an antigen. The candidate solutions in the population, which are represented by vectors consisting of real numbers, are sorted according to their fitness values and then the best n candidates are cloned proportionally with the fitness value. The number of the clones belonging to each candidate is computed as follows:

$$C_i = round\left(\frac{\beta N}{i}\right), \tag{13}$$

where β is the scaling factor and i is the sequence number of the best n candidates. The candidate with a better fitness value is copied a higher number of times, while the candidate with a worse fitness value is copied less. The mutation is also applied to the clones depending on the fitness value in such a manner that the candidate with a better fitness value is less mutated and the candidate with a worse fitness value is more mutated. Finally, the clones are evaluated according to the fitness value and the best clones are included in the next generation. This loop is continued until the terminating condition is reached.

5. The proposed method

In the previously mentioned fuzzy logic-based methods, a fuzzy inference system is usually used as a part of other specific methods, such as the diffusion or wavelet transform approaches. In these approaches, a fuzzy inference system is commonly used for coefficient adjusting. However, a standalone fuzzy inference system can be used as a noise filter for digital images provided that the appropriate training datasets that are obtained from the training images are used [22–27]. Once noisy training image data are applied as input to the fuzzy inference system, the difference between the fuzzy inference system output and the desired output (noise-free training image data) can be made minimal by means of an optimization algorithm. With the help of a trained fuzzy inference system, the noise-free image can be obtained from a noisy image when the difference is close to 0, i.e. appropriate fuzzy system parameters are accurately found by an optimization algorithm. Finding optimal fuzzy system parameters is very difficult if not impossible. However, small difference values can also provide sufficiently optimal results in many applications.

5.1. Training of the fuzzy inference system

The relation between the fuzzy inference system's input and output is determined by membership functions that are used for input fuzzification. In the training phase of the fuzzy inference system, the parameters of the fuzzy rule set membership functions are optimized with the training data. The fuzzy system parameters in the proposed fuzzy filter are optimized by the CSOA with a rule-based style, where the parameters of the fuzzy system are separated according to the rules and only the parameters belonging to the current rule are optimized in each epoch [26]. The training setup is shown in Figure 2 and the output of the fuzzy system converges to the original noise-free training image when the training is done.

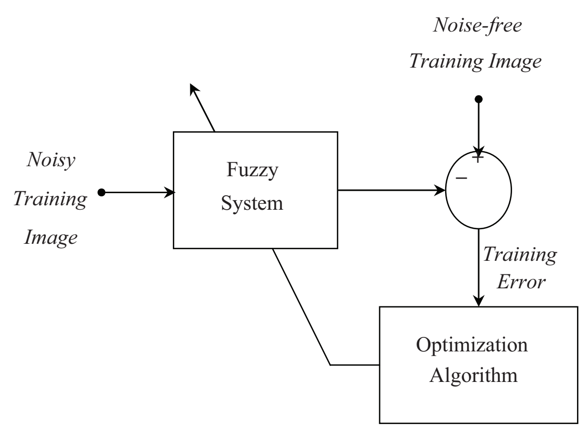

Figure 2. Training of the fuzzy system.

The fuzzy inference system used in the proposed fuzzy filter has 5 inputs and 1 output. The fuzzy rule base includes 10 rules, and the number of rules in the fuzzy system rule base is chosen heuristically and verified experimentally; nevertheless, it can be greater or less than 10. On the other hand, the experimental results indicate that increasing the number of rules slightly improves the performance of the proposed fuzzy filter but also increases the training duration as well as the system complexity. Therefore, the number of rules should be carefully selected to observe a balance between the performance and the system complexity.

The fuzzy filter-based methods were successfully used for impulse noise removal under various digital imaging conditions [22–27]. In a digital image, the impulse noise changes some pixel values to 0 or 255, while all of the pixel values are changed by the speckle noise within a specific range depending on the noise intensity. Therefore, the determination of appropriate training images is very important for forming a fuzzy-based filter specifically for speckle noise. The training images must be designed to include both uniform areas and edges with different gray-level values; hence, variously shaped artificial images can be used. The noisy training image is obtained from a noise-free training image by adding speckle noise with specific noise intensity. When the fuzzy inference system is trained with this pair of images, it can be used as a speckle noise removal operator for any speckled image.

The training images used in this work are artificially generated on a computer and are shown in Figures 3a and 3b. The image in Figure 3a is the noise-free training image, which has a size of 120 $\times$ 120 pixels, and each square box in this image has a size of 8 $\times$ 8 pixels with the same luminance value, which is a uniformly distributed random integer number between 0 and 255. The noisy training image shown in Figure 3b is obtained by corrupting the original noise-free training image by speckle noise with a variance of 0.04. This variance value is not very critical for the fuzzy system training process; nevertheless, experimental observations indicate that the best filtering result is obtained when the noise variance of the noisy input image is close to the noise variance of the noisy training image. Since it is impossible to know exactly the noise variance of the noisy image in practice, the noise variance value of the noisy training image is determined experimentally without selecting very low or high values.

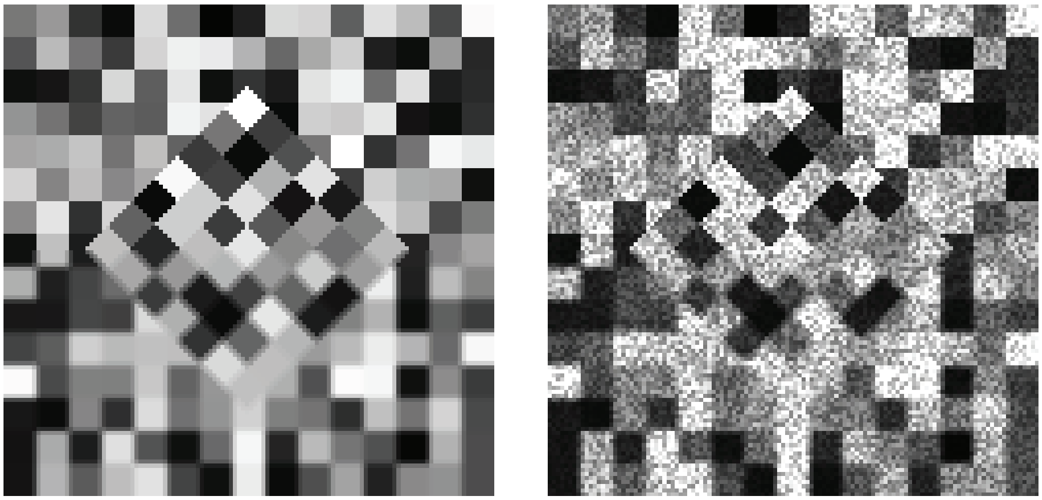

Figure 3. a) Original noise-free training image. b) Noisy training image.

The training data used in the training phase are obtained from the training images by considering a specific neighborhood arrangement. The specific pixel neighborhood in the filtering window of the proposed fuzzy filter is shown in Figure 4a and its application to the fuzzy inference system is shown in Figure 4b. The training input data (I_{TN}), which are applied to the fuzzy system as input, are obtained from the pixel luminance values of the noisy training image, while the training output data (I_{TO}), which are compared with the fuzzy system output, are obtained from the noise-free training image pixel luminance values. The fuzzy inference system used in the proposed method has 5 inputs and 1 output; therefore, 5 input values are acquired from the noisy training image according to specific neighborhood arrangement and 1 desired output value is acquired from the center pixel value of the filter window in the noise-free training image. Many different neighborhood combinations are possible in the filtering window; however, extensive experiments indicate that the best filtering performance is obtained by the proposed neighborhood arrangement in Figure 4a.

not used	*I(m-1,n)*	*not used*
I(m,n-1)	*I(m,n)*	*I(m,n+1)*
not used	*I(m+1,n)*	*not used*

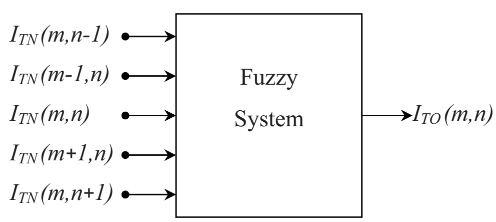

Figure 4. a) Filtering window of the proposed fuzzy filter. b) Application of the filtering window to the fuzzy system.

5.2. The proposed fuzzy filter

A noise removal operation can generally be a problem in luminance transition areas and can lead to blurring or edge distortion during the filtering process. The pixel values in uniform areas away from the edges are less affected by the filtering process, whereas the pixel values in the vicinity of the edges are affected more. Since the edges include useful information, edge distortions make the understanding and interpretation of an image more complicated. In a filtering process, the noise has to be removed from digital images by utilizing the edge information for quality results; therefore, a denoising method has to be edge-sensitive.

The structure of the proposed fuzzy filter is shown in Figure 5. In fact, the application of the trained fuzzy filter on the noisy input image for a one-time performance is sufficient for a reasonable speckle noise removal; however, the proposed fuzzy filter is applied an additional time to improve the performance, especially for the uniform areas of the noisy image. The use of the trained fuzzy system for a second time provides more smoothening, which has useful effects for the uniform areas but leads to smoothing of the edges at the same time. To protect the edges from this smoothing, the regions in the vicinity of the edges are detected by an edge detection and dilation unit, and fuzzy system outputs are used for these regions in the restored image.

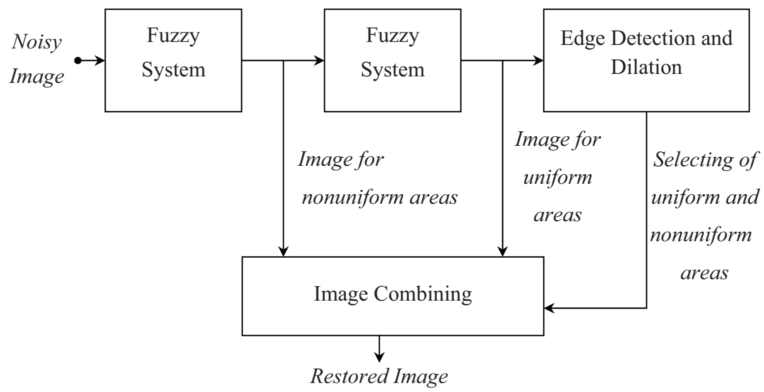

Figure 5. The proposed fuzzy filter.

5.2.1. The edge detection and dilation unit

The edges in any digital image can be found easily using any differential mask kernel. However, finding edges in a noisy image is not easy, because the noise creates extra edges due to changing pixel values in the image. Since the fuzzy filter used in the proposed method already removes the speckle noise, any simple edge detection approach can be used for finding the edges. In the proposed method, the Sobel edge detector kernels, which are column and row kernels, are found to be sufficient for detecting vertical and horizontal edges, respectively. The Sobel method, which is one of the most common edge detection approaches, is based on the central difference in the kernel [36]. In the uniform areas, the differential kernels give a 0 luminance value for the center pixel; however, the luminance value approaches 255 in the vicinity of the edges. After the corresponding edge magnitudes of all of the pixels in the input image are found, the edge image, where the pixel values can assume either 0 or 255, is obtained by applying a threshold to the edge image.

In the proposed method, the dilation operator is used for detecting the vicinity of the edges in the image. The dilation process is gradually applied to the edge image twice, using a 3×3 mask for finding regions close to edges, and the regions revealed after each dilation process are used to determine the transition area of the pixel values of the restored image by means of the 2 filtered noisy image outputs.

5.2.2. The image combiner

The edge image and its dilated forms are used to determine the filtered noisy image output (fuzzy system output) that will be used for the current pixel in the restored image. The edge regions in the restored image are obtained from the once-filtered noisy image output, while the areas remaining after edge dilation in the restored image are filled with the twice-filtered noisy image output. The pixel values of the dilated regions outside of these areas are computed by averaging of the once- and twice-filtered noisy image outputs. The contribution of the once-filtered noisy image output is more in the first dilated region, whereas the contribution of the twice-filtered noisy image output is more in the second dilated region. Experimental results indicate that performance of the fuzzy filter is significantly increased with this approach.

6. Results

The proposed fuzzy filter is tested on various speckled images, which are generated by corrupting popular test images (Lena, Bridge, and Boats) in the literature with multiplicative noise. This type of corruption affects the image in such a manner that uniformly distributed random values with a zero mean and specific variance are multiplied by pixel values of the original noise-free image and then the product values are added to the noise-free image pixel values. In this work, 3 different test images are used and each of them is corrupted by speckle noise with 3 different intensities of variation to obtain speckled noisy test images.

Comparisons are made between the proposed fuzzy filter method and other state-of-the-art methods, including the Lee MMSEF, FROSTF, ADF, SRADF, and Lee ISF, plus 2 classical methods including the mean filter (MF) and the median filter (MEDF). The main criterion in making comparisons between speckle noise filters is that the edges and other details should be preserved during the noise removal process. The comparisons are based on the MSE calculated for the output images of the competing operators, which is defined for 2D gray-scale images as follows:

$$\mathrm{MSE} = \frac{1}{XY}\sum_{x=1}^{X}\sum_{y=1}^{Y}\left(I(x,y) - \widehat{I}\,(x,y)\right)^2, \tag{14}$$

where X and Y are the size of the image, x and y are the pixel positions in the image, and I and $\widehat{I}$ denote the original noise-free image and the restored image, respectively.

Protection of the edges and details in a noisy image is very critical for recognition of the objects in the image that contain useful information for many applications. Some of the noise filters, such as MF and MEDF, can slightly reduce the speckle noise effect, but the edges and details are also destroyed in the filtered output images. The Lee ISF, which is proposed for removing the speckle noise in SAR data, is very successful for SAR data, but its performance is quite dependent on the number of looks and the noise variation. The Lee MMSEF and the FROSTF can reduce speckle effect provided that appropriate filter coefficients are selected according to noisy images. The coefficient in the Lee MMSEF represents the ratio between the variation and mean of the uniform areas in the image, while the coefficient in the FROSTF represents the damping factor. On the other hand, a coefficient value that works very well for a given noisy image may not yield satisfying results for another noisy image. Hence, coefficient adjustment may not be sufficient alone for obtaining good results. The ADF and the SRADF can significantly reduce speckle noise using the anisotropic diffusion technique. The SRADF is similar to the ADF; nevertheless, in the SRADF, a coefficient of the variation is used, as in the Lee MMSEF. In both methods, appropriate filter coefficients should be accurately determined according to the noisy image for maximum filtering performance.

In this work, various neighborhood topologies and various training images are examined for the best filtering performance and the proposed neighborhood topologies and training images are produced for obtaining sufficient results. However, the performance of the fuzzy filter can be increased depending on the training image and/or neighborhood topologies in the filtering window. In addition, selection of the optimization algorithm can be very critical for the fuzzy system parameter optimization in the training phase. The maximum filtering performance can be obtained by finding the optimum fuzzy system parameter values with the appropriate optimization algorithm considering the training data.

The MSE values for the outputs of the competing operators are obtained by extensive experiments and are listed in Table 1 for test images with speckle noise variances (σ) of 0.01, 0.04, and 0.07. The averaged MSE values of the filter outputs with varying noise intensities are listed in Table 2. The best filtering performance is exhibited by the proposed method for various images for various noise intensities. For a visual evaluation, Figures 6a–6j show the filter outputs of the operators for the Lena image corrupted by a 0.05 variation in the noise intensity. This figure also confirms the results presented in the tables and demonstrates that the proposed operator exhibits superior filtering performance over competing operators from the literature.

Figure 6. a) Original Lena image. b) Speckled Lena image with a 0.05 variation in the noise intensity. c) Output of the MF. d) Output of the MEDF.

Figure 6. e) Output of the Lee MMSEF. f) Output of the Lee ISF. g) Output of the FROSTF. h) Output of the ADF. i) Output of the SRADF. j) Output of the proposed filter.

Table 1. MSE values of the operators for the Lena, Bridge, and Boats images corrupted by speckle noise with variations of 0.01, 0.04, and 0.07 in the noise intensities.

	Lena			Bridge			Boats		
Operators	$\sigma = 0.01$	$\sigma = 0.04$	$\sigma = 0.07$	$\sigma = 0.01$	$\sigma = 0.04$	$\sigma = 0.07$	$\sigma = 0.01$	$\sigma = 0.04$	$\sigma = 0.07$
Noisy image	120.1	471.8	808.6	153.2	581.6	984.9	191.5	766.0	1325
MF	134.4	171.3	206.6	199.2	251.3	298.4	179.2	237.2	296.1
MEDF	125.7	231.3	338.0	202.6	332.2	451.2	186.5	353.9	525.5
Lee MMSEF	256.9	153.5	263.3	455.1	287.3	420.4	483.8	233.4	380.7
Lee ISF	332.8	146.3	362.6	346.6	282.4	538.4	653.2	213.6	571.2
FROSTF	117.5	154.0	190.0	187.2	237.7	284.5	163.9	220.7	280.9
ADF	173.3	178.9	189.7	293.4	297.1	310.8	222.8	229.5	249.7
SRADF	127.3	130.0	131.9	358.6	364.2	367.8	233.9	230.8	229.4
Proposed FF	75.4	97.0	130.6	192.7	202.7	250.1	137.9	165.8	216.3

Table 2. Average MSE values of the operators' outputs for all of the speckle noisy test images with variations of 0.01, 0.04, and 0.07 in the noise intensities.

Methods	Average MSE values of the 3 images			Total average
	$\sigma = 0.01$	$\sigma = 0.04$	$\sigma = 0.07$	
Noisy image	154.9	606.4	1039.0	600.1
MF	170.9	219.9	267.0	219.2
MEDF	171.6	305.8	438.2	305.2
Lee MMSEF	398.6	224.7	354.8	326.0
Lee ISF	444.2	214.1	490.7	383.0
FROSTF	156.2	204.1	251.8	204.0
ADF	229.8	235.1	250.1	238.3
SRADF	239.9	241.6	243.0	241.5
Proposed FF	135.3	155.1	199.0	163.1

7. Conclusion

A novel fuzzy filter for speckle noise removal based on a fuzzy inference system has been presented. The proposed fuzzy filter significantly removes speckle noise while effectively preserving the edges. The main advantage of the proposed filter is that it assumes no predetermined coefficient values, unlike most other operators in the literature. It has been concluded that the proposed filter significantly reduces speckle noise from images while preserving edges and it can be used as an effective tool for speckle noise removal.

Acknowledgment

This work was supported by TÜBİTAK under project number 110E051.

References

[1] J.W. Goodman, "Some fundamental properties of speckle", Journal of the Optical Society of America, Vol. 66, pp. 1145–1150, 1977.

[2] A.N. Jain, Fundamentals of Digital Image Processing, Upper Saddle River, NJ, USA, Prentice Hall, 1989.

[3] Y. Yu, S. Acton, "Speckle reducing anisotropic diffusion", IEEE Transactions on Image Processing, Vol. 11, pp. 1260–1270, 2002.

[4] J.S. Lee, "Digital image enhancement and noise filtering by using local statistics", IEEE Transactions on Pattern Analysis, Vol. 2, pp. 161–168, 1980.

[5] V.S. Frost, J.A. Stiles, K.S. Shanmugan, J.C. Holtzman, "A model for radar images and its application to adaptive digital filtering of multiplicative noise", IEEE Transactions on Pattern Analysis, Vol. 4, pp. 157–165, 1982.

[6] D.T. Kuan, A.A. Sawchuk, T.C. Strand, P. Chavel, "Adaptive noise smoothing filter for images with signal-dependent noise", IEEE Transactions on Pattern Analysis, Vol. 7, pp. 165–177, 1985.

[7] D.T. Kuan, A.A. Sawchuk, T.C. Strand, P. Chavel, "Adaptive restoration of images with speckle", IEEE Transactions on Acoustics, Speech and Signal Processing, Vol. 35, pp. 373–383, 1987.

[8] R. Wallis, "An approach to the space variant restoration and enhancement of images", Proceedings of the Image Science Mathematics Symposium, pp. 107–111, 1976.

[9] A. Lopes, R. Touzi, E. Nezry, "Adaptive speckle filters and scene heterogeneity", IEEE Transactions on Geoscience and Remote Sensing, Vol. 28, pp. 992–1000, 1990.

[10] A. Lopes, E. Nezry, R. Touzi, H. Laur, "Structure detection and statistical adaptive speckle filtering in SAR images", International Journal of Remote Sensing, Vol. 14, pp. 1735–1758, 1993.

[11] P. Perona, J. Malik, "Scale space and edge detection using anisotropic diffusion", IEEE Transactions on Pattern Analysis, Vol. 12, pp. 629–639, 1990.

[12] K. Krissian, C.F. Westin, R. Kikinis, K. Vosburgh, "Oriented speckle reducing anisotropic diffusion", IEEE Transactions on Image Processing, Vol. 16, pp. 1412–1424, 2007.

[13] K. Krissian, "A new variational image restoration applied to 3D angiographies", IEEE Workshop on Variational and Level Set Methods in Computer Vision, pp. 65–72, 2001.

[14] K. Krissian, "Flux-based anisotropic diffusion applied to enhancement of 3D angiogram", IEEE Transactions on Medical Imaging, Vol. 21, pp. 1440–1442, 2002.

[15] S.A. Fernandez, L.C. Alberola, "On the estimation of the coefficient of variation for anisotropic diffusion speckle filtering", IEEE Transactions on Image Processing, Vol. 15, pp. 2694–2701, 2006.

[16] J.S. Lee, J.H. Wen, T.L. Ainsworth, K.S. Chen, A.J. Chen, "Improved sigma filter for speckle filtering of SAR imagery", IEEE Transactions on Geoscience and Remote Sensing, Vol. 47, pp. 202–213, 2009.

[17] J.S. Lee, "Digital image smoothing and the sigma filter", Computer Vision, Graphics, and Image Processing, Vol. 24, pp. 255–269, 1983.

[18] J.S. Lee, "A simple speckle smoothing algorithm for synthetic aperture radar images", Transactions on Systems, Man, and Cybernetics, Vol. 13, pp. 85–89, 1983.

[19] P. Puvanathasan, K. Bizheva, "Interval type-II fuzzy anisotropic diffusion algorithm for speckle noise reduction in optical coherence tomography images", Optics Express, Vol. 17, pp. 733–746, 2009.

[20] P. Puvanathasan, K. Bizheva, "Speckle noise reduction algorithm for optical coherence tomography based on interval type-II fuzzy set", Optics Express, Vol. 15, pp. 15747–15758, 2007.

[21] Y. Zhang, H.D. Cheng, J. Tian, J. Huang, X. Tang, "Fractional subpixel diffusion and fuzzy logic approach for ultrasound speckle reduction", Pattern Recognition, Vol. 43, pp. 2962–2970, 2010.

[22] M.E. Yuksel, E. Besdok, "A simple neuro-fuzzy impulse detector for efficient blur reduction of impulse noise removal operators for digital images", IEEE Transactions on Fuzzy Systems, Vol. 12, pp. 854–865, 2004.

[23] M.E. Yuksel, "A hybrid neuro-fuzzy filter for edge preserving restoration of images corrupted by impulse noise", IEEE Transactions on Image Processing, Vol. 15, pp. 928–936, 2006.

[24] M.T. Yildirim, A. Basturk, M.E. Yuksel, "Impulse noise removal from digital images by a detail-preserving filter based on type-2 fuzzy logic", IEEE Transactions on Fuzzy Systems, Vol. 16, pp. 920–928, 2008.

[25] Y. Yüksel, M. Alçı, M.E. Yüksel, "Performance enhancement of image impulse noise filters by image rotation and fuzzy processing", AEU - International Journal of Electronics and Communications, Vol. 64, pp. 329–338, 2010.

[26] M.A. Soyturk, A. Basturk, M.E. Yuksel, "Rule based optimization of type-2 fuzzy inference system used at impulse noise removing", 19th IEEE Conference on Signal Processing and Communications Applications, pp. 833–836, 2011.

[27] M.E. Yuksel, A. Basturk, "Application of type-2 fuzzy logic filtering to reduce noise in color images", IEEE Computational Intelligence Magazine, Vol. 7, pp. 25–35, 2012.

[28] M. Amirmazlaghani, H. Amindavar, "A novel sparse method for despeckling SAR images", IEEE Transactions on Geoscience and Remote Sensing, Vol. 50, pp. 5024–5032, 2012.

[29] M.R. Hajiaboli, "An anisotropic fourth-order diffusion filter for image noise removal", International Journal of Computer Vision, Vol. 92, pp. 177–191, 2011.

[30] I. Elamvazuthi, M.L.B.M. Zain, K.M. Begam, "Despeckling of ultrasound images of bone fracture using multiple filtering algorithms", Mathematical and Computer Modelling, Vol. 57, pp. 152–168, 2013.

[31] B. Huang, P. Bu, X. Wang, N. Nan, X. Guo, "Speckle reduction in parallel optical coherence tomography by spatial compounding", Optics & Laser Technology, Vol. 45, pp. 69–73, 2013.

[32] H. Chen, Y. Zhang, H. Wang, C. Ding, "Stationary-wavelet–based despeckling of SAR images using two-sided generalized gamma models", IEEE Transactions on Geoscience and Remote Sensing, Vol. 9, pp. 1061–1065, 2012.

[33] S.H.C. Ortiz, T. Chiu, M.D. Fox, "Ultrasound image enhancement: a review", Biomedical Signal Processing, Vol. 7, pp. 419–428, 2012.

[34] J.S.R. Jang, "ANFIS: adaptive-network-based fuzzy inference system", IEEE Transactions on Systems, Man, and Cybernetics, Vol. 23, pp. 665–684, 1993.

[35] J.E. Hunt, D.E. Cooke, "Learning using an artificial immune system", Journal of Network and Computer Applications, Vol. 19, pp. 189–212, 1996.

[36] L.G. Shapiro, G. Stockman, Computer Vision, Upper Saddle River, NJ, USA, Prentice Hall, 2001.